Progress in Medical Devices
eISSN: 2957-5478

Zentime

Research Article https://doi.org/10.61189/061485jysfwu

Impact of tissue-electrode contact force on irreversible electroporation for atrial fibrillation in potato models

Tiantian Hu, Yingfan Yuan, Mengying Zhan, Binyu Wang, Lin Mao, Yu Zhou

School of Health Science and Engineering, University of Shanghai for Science and Technology, Shanghai 200093, China.

Corresponding author: Yu Zhou.

Acknowledgements: This work was financially supported by National Natural Science Foundation of China (51901137).

Declaration of conflict of interest: None.

Received August 22, 2023; Accepted November 28, 2023; Published December 31, 2023

Highlights

- A strong positive correlation was identified in the investigation of the relationship between contact force and irreversible electroporation (IRE) efficacy for tissue ablation.
- This research conducted on potato models highlights the importance of optimizing electrode contact force in IRE for applications in atrial fibrillation treatment.
- Our findings provide insights into the design of advanced IRE ablation protocols and facilitate the clinical development and translation of this technology for effective atrial fibrillation treatment.

Abstract

Background: Irreversible electroporation (IRE) is an emerging tissue ablation technique that offers advantages over traditional catheter ablation, such as minimal thermal damage and reduced treatment time. However, as this technique also involves delivering energy through a catheter to target tissue, there are still challenges regarding the contact between the catheter and the targeted tissue, and there is a lack of relevant studies. In this study, we examined this issue using potato models with three groups of experiments. **Methods:** First, the relationship between the effect of biphasic and monophasic output modes and contact force (CF) was studied. Next, the effect of different voltages on biphasic output mode was examined. Finally, impedance analysis was conducted to test the contact impedance under different CFs. **Results:** The IRE ablation efficacy increased with the increase of CF in both monophasic and biphasic output modes, and there was a strong correlation between the ablation efficacy and the CF. In addition, at three voltage levels, the IRE ablation efficacy increased with increasing CF, and there was a strong correlation between the ablation efficacy and the CF. **Conclusion:** The results indicate that, under common IRE electrical parameter configuration, the effect of IRE on the tissue has a positive response to the CF of the electrode in the potato model. This finding has important implications for the design of electrodes used in IRE for the treatment of atrial fibrillation.

Keywords: Irreversible electroporation ablation, tissue-electrode contact force, atrial fibrillation, catheter ablation, potato

Introduction

Atrial fibrillation (AF) is a prevalent cardiac arrhythmia, affecting up to 4% of the global population. While the incidence of AF in individuals under 40 is very low (less than 1%), it drastically elevates with the increase of age, affecting 17% of individuals over 80 years old [1]. This escalating prevalence in older individuals poses a significant challenge to the extension of life expectancy globally. AF not only significantly impacts the body's functioning but also leads to emotional distress and reduced quality of life [2]. It is estimated that by 2050, there will be 6-12 million individuals with AF worldwide, with an estimated 17.9 million people in Europe alone affected by this disease by 2060 [3, 4].

The management of AF involves anticoagulation, rhythm control, and heart rate control

Address correspondence to: Yu Zhou, School of Health Science and Engineering, University of Shanghai for Science and Technology, NO.516 Jungong Road, Shanghai 200093, China. Tel: 18021042556, E-mail: zhouyu@usst.edu.cn.

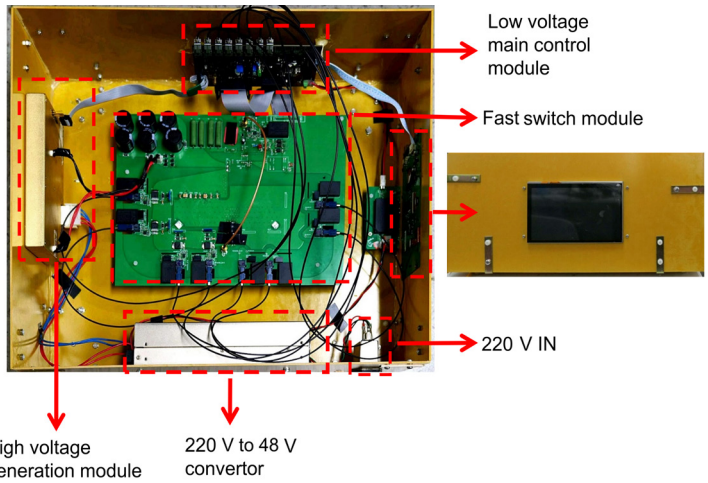

Figure 1. Laboratory prototype pulse generator and its components.

through various means. The most commonly used strategies include medical therapy and catheter ablation [5, 6]. Additionally, lifestyle modifications can also aid in AF management and reduce its incidence [7]. Radiofrequency ablation and Cryoballoon ablation are the main clinical catheter ablation methods for AF. However, both of these catheter ablation techniques rely on temperature transmission, leading to three practical problems. The first problem arises due to blood flow in the target area, causing a heat sink effect that can result in incomplete treatment. The second issue is non-selective killing of cells due to high or low temperature during treatment, which may cause unnecessary thermal damage to tissues adjacent to the target area [8, 9]. Lastly, the treatment efficacy depends on the contact force (CF) between electrode and tissue, leading to incomplete treatment due to the contact problem [9, 10]. Owing to these issues, there is an urgent need for a clinical novel therapeutic modality.

The irreversible electroporation (IRE) causes nanometer-sized irreversible micropores on the cell membrane under the influence of a high-voltage electric field. The presence of these micropores leads a loss of cell homeostasis resulting in cell death. This is the principle behind IRE tissue ablation. This technique was initially used in the industrial and food sectors [11-13], and was later introduced into tumor ablation therapy, where it proved its non-thermal properties and safety. It is now being applied in AF ablation therapy [14-16]. Compared to other catheter ablation techniques, IRE ablation has less thermal damage to surrounding tissues and selectively kills cardiomyocytes [17, 18].

Like radiofrequency ablation and Cryoballoon ablation, IRE ablation also delivers energy to the target tissue via a catheter. Therefore, achieving proper CF remains a challenge [19, 20]. However, the relationship between CF and IRE ablation efficacy is not explicit, and there are few relevant studies [21, 22]. Therefore, further in-depth research is warranted to understand the correlation.

The concept of CF in the field of robotic surgery is a significant and common topic, and the research methods employed in this area hold substantial reference value for this study [23-25]. The aim of this study is to investigate the relationship between CF and IRE ablation efficacy in a potato model and to provide insights into catheter design for IRE ablation of AF. Potato model is a commonly used plant model in IRE ablation experiments due to its capacity for visually representing the effects of IRE ablation. It also offers practical advantages, such as easy access to experimental materials and the absence of ethical concerns [26-28]. This study utilized potato model and initially examined the relationship between CF and the IRE ablation efficacy under both biphasic and monophasic pulse sequences, and then changed the amplitude to evaluate the response of efficacy and CF.

Material and methods

Laboratory prototype pulse generator and its output waveform

The high-voltage pulse generator used in this experiment is a laboratory prototype pulse generator (University of Shanghai for Science and Technology, China). The circuit design is based on the H-bridge biphasic pulse generator using MOSFETs (G3R30MT12J, GeneSiC Inc., USA) with the ability to withstand 1200 V. The generator can output monophasic and biphasic pulses up to 2000 V with a pulse repetition rate of up to 800 Hz. The duration of the output pulse is about 800 ns, providing a waveform output that meets the experimental requirements. The generator comprises a human-computer interface, a high-voltage generation module, an alternating current to direct current module, a fast-switch module, and a low-voltage control module, as illustrated in **Figure 1**.

In the first experiment, we delivered two IRE pulse sequences: a monophasic pulse sequence and a biphasic pulse sequence, as illustrated in **Figure 2**. The monophasic pulse

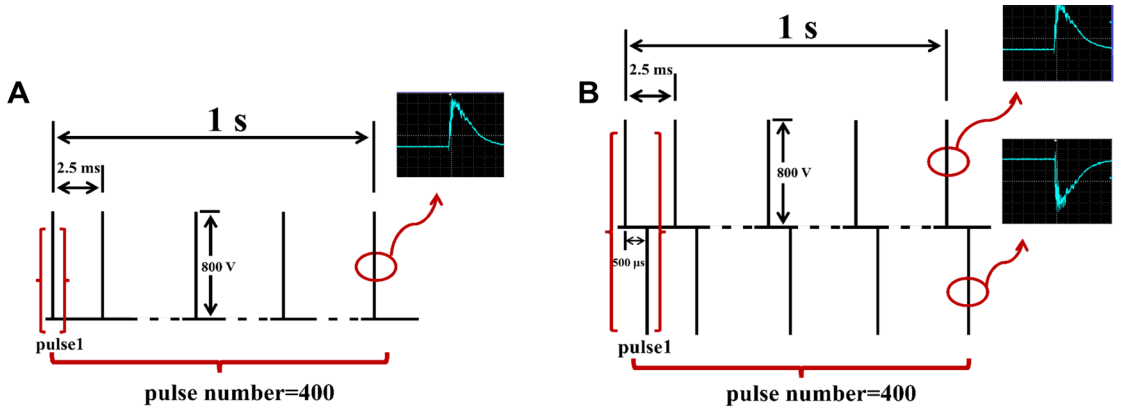

Figure 2. Two representative types of output waveform for the pulse generator. (A) Representative biphasic pulse; (B) Representative monophasic pulse.

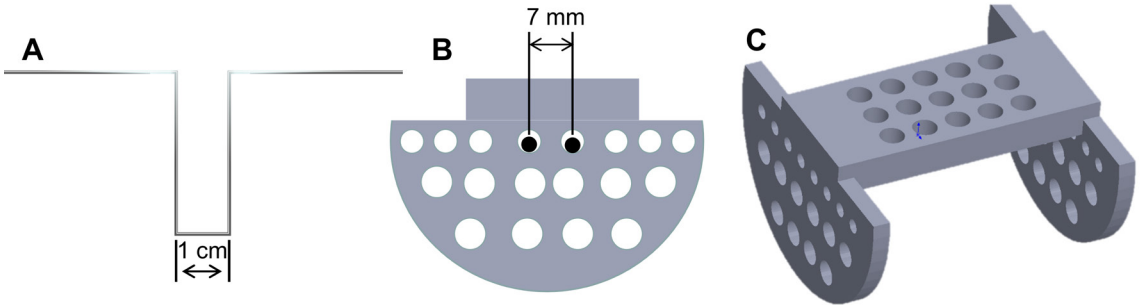

Figure 3. Design schematic of the electrode and its clamp. (A) Front view of the electrode; (B) Side view of the electrode clamp; (C) 3D design schematic of the electrode clamp.

sequence consisted of 3,000 monophasic pulses, with an amplitude of 800 V, a pulse width of 800 ns, and a repetition rate of 400 Hz (**Figure 2A**). The biphasic pulse sequence comprised 3000 biphasic pulses, with an amplitude of 800 V, a pulse width of 800 ns, a repetition rate of 400 Hz, and a biphasic interval of 500 μs (**Figure 2B**). To investigate the relationship between CF and IRE ablation at different voltages, we conducted experiments with 800 biphasic pulses, using amplitudes of 350 V, 500 V, and 800 V, a pulse duration of 800 ns, a repetition rate of 400 Hz, and a biphasic interval of 500 μs.

Electrode design and its clamp

Due to the presence of inherent variability in each potato model and the potential induction of artificial errors during processing, the resultant effect plane of the models cannot remain entirely parallel to the electrode plane, thereby causing an incongruity in the contact area between the electrode and the divergent model surfaces of multiple potatoes. To mitigate this inconsistency, we shortened the length of the contact part between the electrode and the potato model. This approach lessens the dependency of the experimental results on the parallel relationship between the potato models' action surface and the electrode plane.

The electrode, as shown in **Figure 3A**, is made of 304 stainless steel with a convex pattern that allows only partial of the electrode to contact with the potato model during pulse delivery. The diameter of the electrode is 0.7 mm. The length of the contact area between the electrode and the potato model was set to be 1 cm.

The electrode clamp used in this experiment was a white PLA 3D printed model. It is equipped with holes of different sizes on the side to accommodate fixed electrodes of varying sizes and allow for adjustment of the distance between two electrodes as required, which is set at 0.7 cm in this study, as presented in **Figures 3B and C**. The clamps are secured in place using screws and can be mounted onto a lifting platform.

Process of the potato models and assessment of the efficacy

Potatoes have been used as a common plant

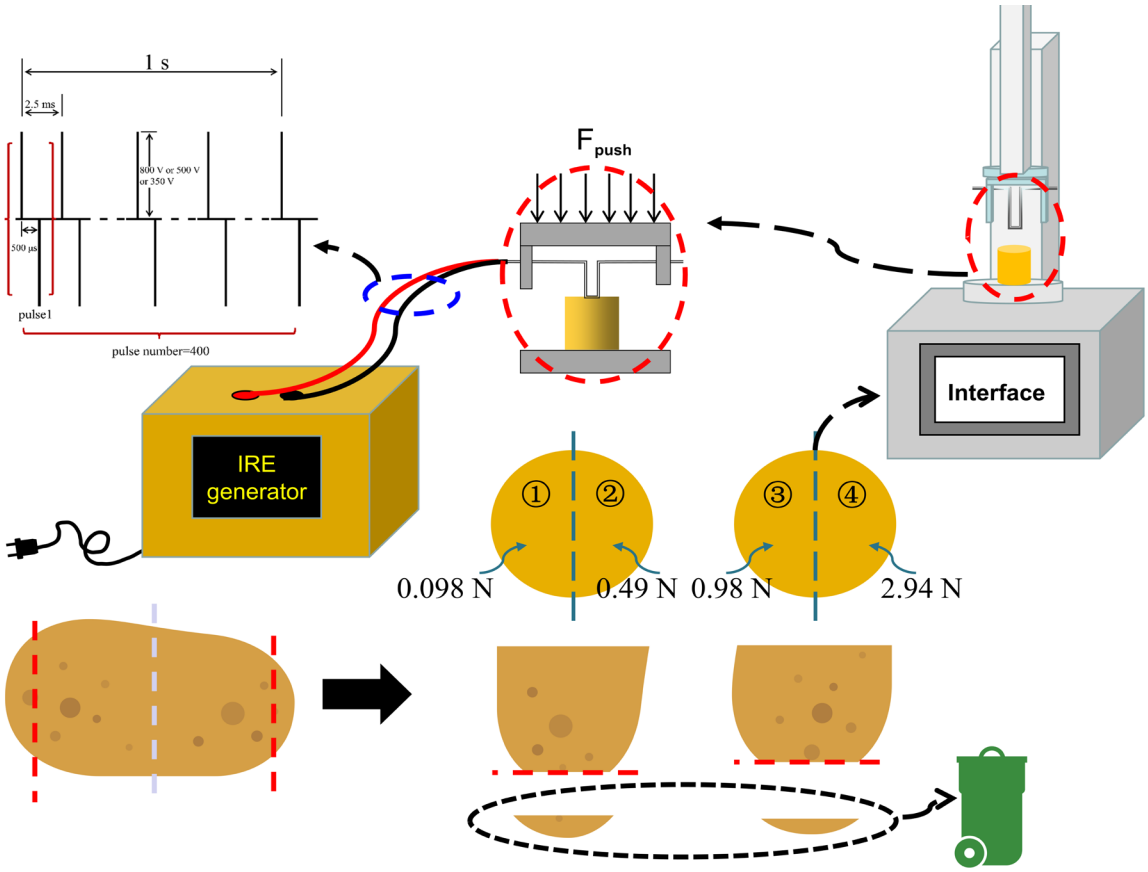

Figure 4. Schematic diagram of potato processing method and experimental steps. IRE, irreversible electroporation.

model in IRE experiments to verify the efficacy of pulses, evaluate the efficacy of novel electrodes, and measure the superiority of pulse sequences [26-28]. Due to the advantages of low cost, easy evaluation of results, and no ethical issues, it is widely used in IRE research [26-28]. Typically, black areas of melanin accumulation arising from intracellular polyphenol oxidation can only be observed in the potato model 12 to 48 h after the experiment is conducted. The results are evaluated using comparisons among the black metrics under various parameters, which is a convenient, fast, and economical method for hypotheses testing [26]. Other evaluation methods, such as MRI scan and TTC staining, are also available [26, 29].

In this experiment, we employed direct observation to assess the validity of the experimental results. To ensure the experiment's validity and eliminate the interference of factors such as individual variability and tissue uniformity, a potato model is cut into 2 pieces. Each piece is divided into 2 regions. And on each region, we applied different CF with the same pulse. The potato processing method and experimental procedure are presented in **Figure 4**. The potatoes used in this experiment were procured from a nearby supermarket (RT-Mart, China) and utilized within 4 h of procurement. To observe the output waveform, an oscilloscope (AFG3022B, Tektronix Inc., USA) was used in all experiments. Impedance was detected using an impedance analyzer (IM3570, Hioki Inc., Japan).

Pressure control lifting platform

To regulate the CF output, a pressure-controlled lifting platform, manufactured in our laboratory, was employed in this study. This platform comprises a motor-driven arm, a control module, and a human-computer interface, as illustrated in **Figure 5**. Using PID control outputs, the device could output various pressures up to 70 N, while pressure data were sampled using the AD5933 (Analog Inc., USA). In the experiment, we set the CF to 0.098 N (10 g), 0.49 N (50 g), 0.98 N (100 g), and 2.94 N (300 g), respectively, with G taking a value of 9.8 m/s^2.

Overview of experimental design

The study comprised three experiments, using a total of 55 potato models. The first experiment (20 potato models) examined the relationship between CF (0.098 N, 0.49 N, 0.98 N, and 2.94 N) and IRE ablation efficacy under

Table 1. ANOVA Test Results for one-way repeated measures under different output modes

Output mode	F	P-value	matching F	Matching P-value
Monophasic	23.75	2e-7***	2.993	2e-3**
Biphasic	22.94	2e-9***	13.05	1e-10***

Note: **P<0.01, ***P<0.001.

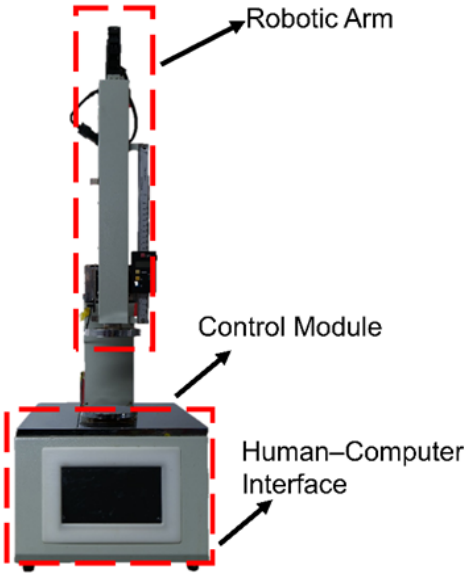

Figure 5. Pressure control lifting platform and its components.

both monophasic and biphasic pulse sequences at the same voltage amplitude. The second experiment (30 potato models) assessed the relationship between CF and IRE ablation efficacy with different output voltage amplitudes (350 V/500 V/800 V). A reference group was set, which was subjected only to CF without pulse (5 potato models). The inclusion of a reference group was intended to exclude mechanical damage caused by the electrode to the potato model and to prevent it from affecting the final experimental results. Prior to commencing with this experiment, a biphasic pulse output mode was confirmed with CF set at 0.098 N, 0.49 N, 0.98 N, and 2.94 N. Finally, 15 potato models were selected from the above experiments to determine the relationship between the impedance and different CF by gradually increasing the CF under the observation of the impedance analyzer.

Image processing

The potato model was photographed using a camera (Lumix S5, Panasonic Inc., Japan) fixed on a tripod, with a constant distance. The image data was processed using MATLAB 2020 (MathWorks Inc., USA). The processing method involved importing the color image into MATLAB and selecting the reference area (potato model's original color) as the benchmark. The RGB value of the color block of reference region was used to set a threshold value of 100. Pixels were considered to belong to the reference region (non-oxidized region) when the difference between the RGB value of the target region and the benchmark RGB value was within the threshold value. Otherwise, the area was categorized as the action region (oxidized region).

Data and Statistical Analysis

Statistical analysis was performed using SPSS software (IBM Inc., USA). Data were expressed as mean ± standard deviation (SD) unless otherwise stated. Oxidation areas of different regions within the single potato in the same experimental group were compared using one-way repeated measures ANOVA. Post hoc pairwise comparisons were conducted using Tukey test (*P<0.05, **P<0.01, ***P<0.001). Pearson's correlation analysis was used to determine the correlation between CF and ablated area within the same potato.

Results

Relationship between CF and IRE ablation efficacy under monophasic pulse and biphasic pulse

In this experiment, 20 potato models were prepared according to the methodology illustrated in **Figure 4** and were subsequently divided into two groups. Each potato model was subjected to four IRE ablation experiments with varying CFs. While keeping the output electrical parameters constant, different pulse output modes (monophasic and biphasic) were employed in each experimental condition. Following the completion of the experiments, all potato models were left for 24 h under room temperature (20 °C), and their results were recorded by a camera. Moreover, all potato models underwent the same after-treatment procedure following the experiment.

The results of the ANOVA test under different output modes are presented in **Table 1**. It was evident that significant differences existed in the mean effects of various CFs for both output modes. Furthermore, there was a significant difference in matching effects under monopha-

Table 2. Turkey Post-hoc Test Results for every two CF under both output modes

	0.098 N & 0.49 N	0.098 N & 0.98 N	0.098 N & 2.94 N	0.49 N & 0.98 N	0.49 N & 2.94 N	0.98 N & 2.94 N
Monophasic	7e-4***	2e-5***	8e-6***	0.94	4.6e-2*	6e-3**
Biphasic	1.9e-3**	8e-6***	1e-9***	0.29	3e-3**	4.5e-2*

Note: *P<0.05, **P<0.01, ***P<0.001. CF, contact force.

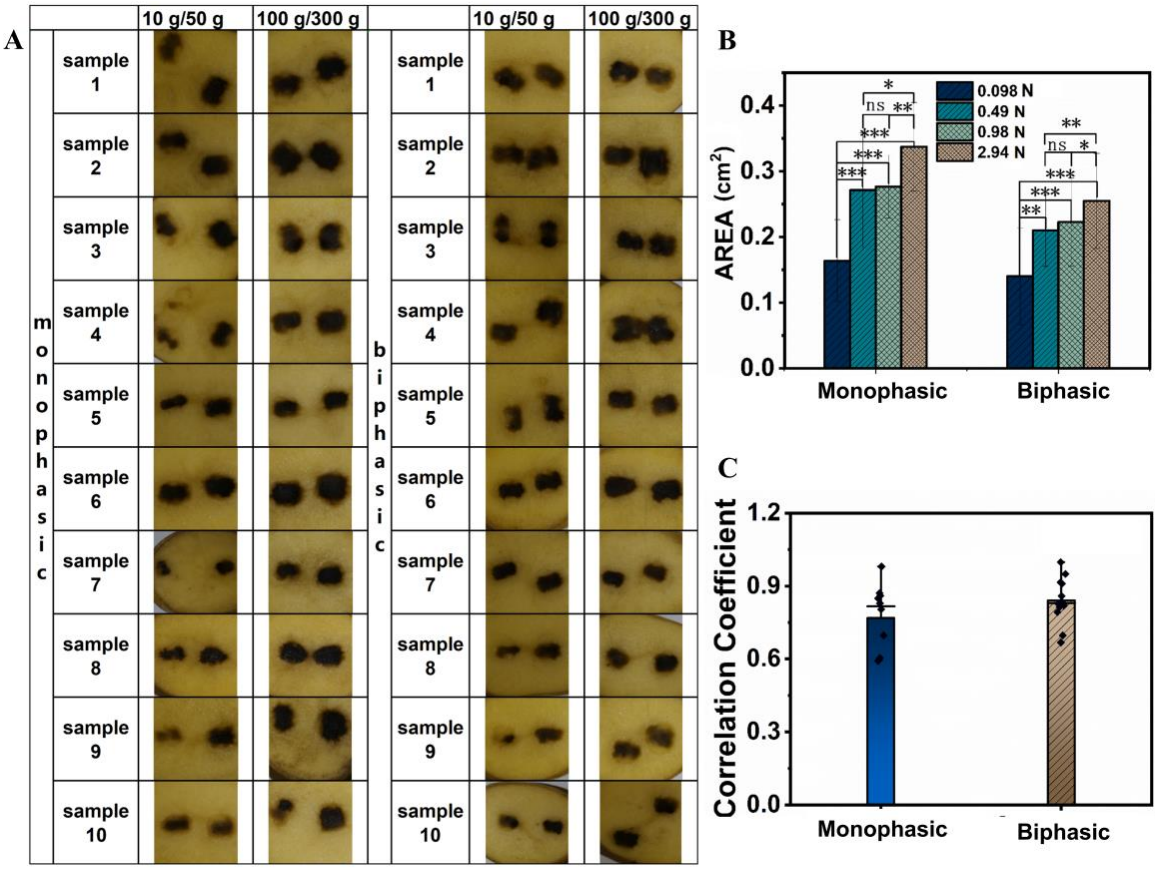

Figure 6. Experimental results and data evaluation in biphasic pulse output mode and monophasic pulse output mode. (A) Experimental results of biphasic and monophasic pulse on potato models; (B) Statistics data showing effect of different output mode on oxidation area under different CFs; (C) Correlation coefficient of CF and oxidation area under different output modes. CF, contact force. *P<0.05, **P<0.01, ***P<0.001; ns represents P>0.05.

sic output and a highly significant difference under biphasic output.

The experimental results of the potato model are shown in **Figure 6A**. After the experiments, surface oxidation areas caused by IRE could be observed on all potato models. **Figure 6B** depicts the relationship between the size of the IRE ablation areas and the CF within the same experimental group. The results of the Turkey post-hoc test are annotated in **Table 2**. It was evident that, regardless of whether monophasic or biphasic modes, there was a highly significant difference in the size of the ablation zone at 0.098 N compared to the other CFs. Under both output modes, there was no significant difference in the size of the ablation zone at 0.49 N and 0.98 N. However, for the 0.49 N and 2.94 N CFs, the size of the ablation zone exhibited an extremely significant difference in the monophasic output mode and a more noticeable difference in the biphasic output mode. Similarly, at the CF of 0.98 N and 2.94 N, there was a highly significant difference in the size of the ablation zone in the monophasic output mode and a significant difference in the biphasic output mode.

Figure 6C illustrates the correlation between CF and IRE ablation areas under both operating modes. The correlation coefficients under both operating modes were greater than 0.5, which implies a robust relationship between the electrode's CF and the ablation effect.

Relationship between CF and IRE ablation with different amplitudes under biphasic pulse

In this experiment, 30 potato models in three groups were ablated using three different

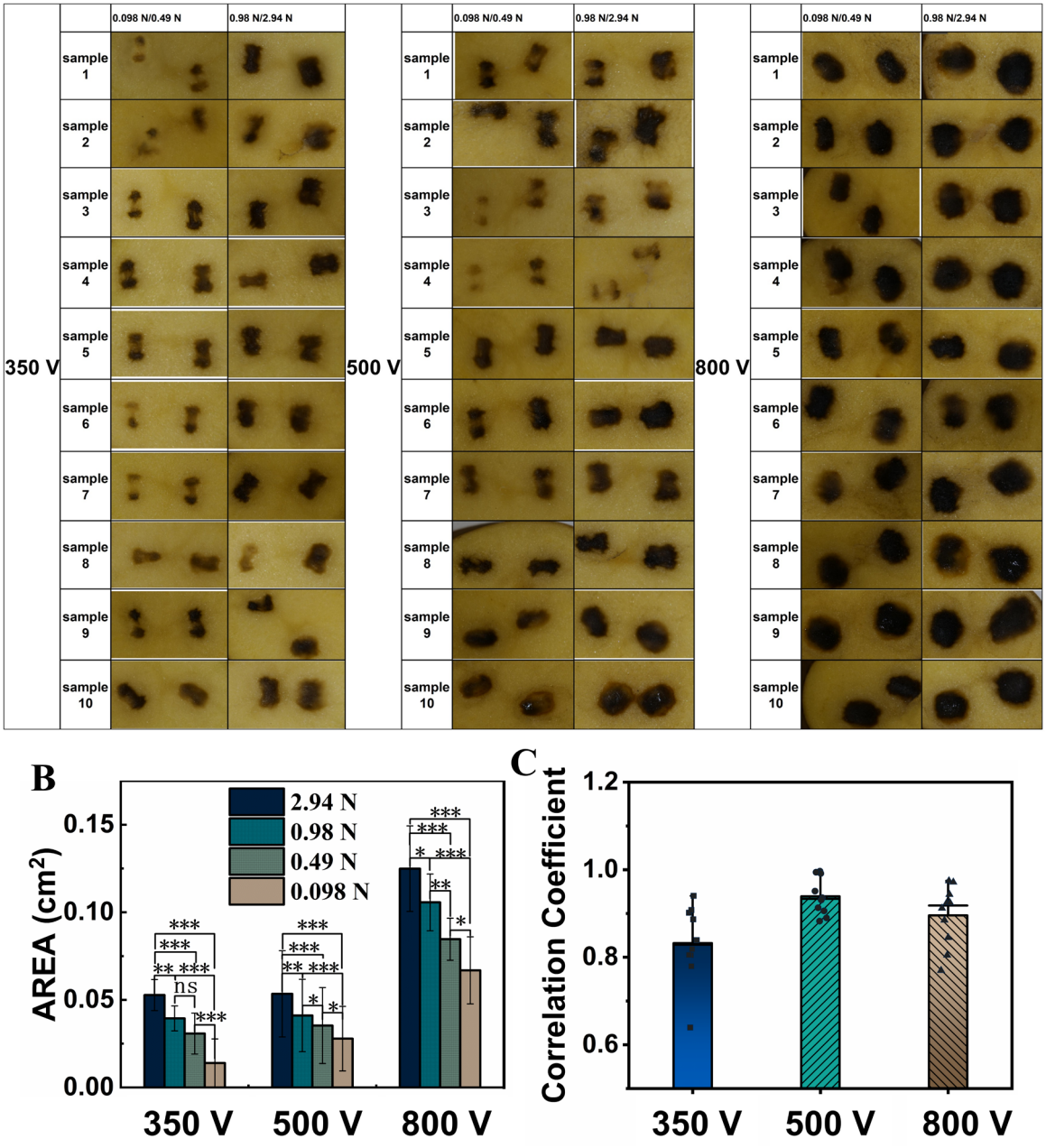

Figure 7. Experimental results and data evaluation in different output amplitudes. (A) Experimental results of the 300V,500V, and 800V groups; (B) Statistics data showing effect of different output amplitudes on oxidation area under different CFs; (C) Correlation coefficient of CF and oxidation area under different output amplitudes. CF, contact force. *P<0.05, **P<0.01, ***P<0.001; ns represents P>0.05.

amplitudes (350 V, 500 V, and 800 V) with the same pulse sequence. IRE ablation experiments were conducted on the cross-sections of each potato model under four different CFs. Subsequently, all potato models were kept at room temperature (20 °C) for 24 h and photographed with a camera. Following the experiment, uniform disposal was performed on all the potato models.

The results of the ANOVA test for different output voltage amplitudes are presented in **Table 3**. It could be observed that, irrespective of the output amplitude, significant differences existed among the various CFs. Furthermore, there was a significant difference in matching effects at a voltage amplitude of 350 V, and a highly significant difference at output voltages of 500 V and 800 V.

The experimental outcomes of the potato model are depicted in **Figure 7A**, which displays visible surface oxidation areas resulting from IRE ablation on all the potato models after the experiment. **Figure 7B** delineates the alteration in the size of IRE ablation areas with respect to CFs applied within the same output voltage. The results of the Turkey post-

Table 3. ANOVA Test Results for one-way Repeated Measures under different output voltages

Output Voltage	F	P-value	matching F	Matching P-value
350 V	35.37	2e-9***	3.074	1.1e-2*
500 V	41.70	3e-10***	54.45	5e-15***
800 V	36.05	1e-9***	4.773	<7e-4***

Note: *P<0.05, ***P<0.001

Table 4. Turkey Post-hoc Test Results for every two CF under three amplitudes

	0.098 N & 0.49 N	0.098 N & 0.98 N	0.098 N & 2.94 N	0.49 N & 0.98 N	0.49 N &2.94 N	0.98 N & 2.94 N
350V	9e-4***	3e-6***	1e-9***	0.138	3e-5***	9e-3**
500V	4.7e-2*	4e-5***	3e-10***	1.3e-2*	4e-8***	2e-4*
800V	2.7e-2*	3e-6***	1e-9***	7e-3**	2e-6***	1.5e-2*

Note: *P<0.05, **P<0.01, ***P<0.001.

hoc test are annotated in **Table 4**. It could be observed that, the oxidation area exhibited a growth trend with increasing CF at the same voltage. At the voltage of 350 V, there was a highly significant difference between 0.098 N and 0.49 N, and a significant difference was also observed at voltages of 500 V and 800 V. At 0.098 N and other two CFs (0.98 N, 2.94 N), all three output voltage amplitudes exhibited significant differences. For the CFs of 0.49 N and 0.98 N, there was no significant difference at 350 V, a significant difference at 500 V, and a more noticeable difference at 800 V. Under the CFs of 0.49 N and 2.94 N, highly significant differences existed for all three output voltage amplitudes. For 0.98 N and 2.94 N CFs, there were noticeable differences at 350 V and 500 V, and a significant difference at 800 V. Moreover, **Figure 7C** reveals the connection between CF and ablation efficacy under varied voltage output conditions. Intriguingly, the correlation coefficients between CF and ablation area were greater than 0.5, indicating a robust relationship between the two variables.

Impedance of potato model under different CFs

The experiment revealed that the contact impedance of various potato models differed under constant CF. An impedance analyzer was utilized to assess the contact impedance of the potato models, and **Figure 8** depicts the differences in contact impedance among the various models under different CFs. Despite the discrepancies observed in the contact impedance among different potato models, an identifiable pattern emerged and was consistent across all the models: an increase in CF corresponded with a decrease in contact impedance.

Discussion

We hypothesized that the CF between the electrode and tissue could potentially influence the effectiveness of IRE treatment. To examine this relationship, experiments were performed on potato models.

To ensure that the experimental outcomes were not influenced by temperature, a thermal imaging camera (323 pro, Fotric Inc., China) was utilized to monitor and record the temperature in real-time during the experiment. The thermal imaging outcomes are depicted in **Figure 9A**. Following the application of pulses, the temperature near the electrode increased maximally to 29.7 °C , which is insufficient to cause cell death. Hence, the impact of temperature on the findings can be disregarded. This finding aligns with previous investigations, indicating that prolonging the biphasic interval beyond 1 ms can drastically reduce thermal damage during the treatment process [30].

To prevent the mechanical damage caused by the CF between the electrode and potato from influencing the tissue, a control group was established. As shown in **Figure 9B**, the control group did not exhibit enzyme-catalyzed browning under varied CF (0.098 N, 0.49 N, 0.98 N, 2.94 N) in the absence of pulse output.

It is important to acknowledge that even though we ensured uniformity in the size and variety of the purchased potatoes, variations in the impedance response among different potato models at the same CF may still exist due to individual differences. The differences in impedance response could be attributed to various factors such as water content, cutting position, or uniformity of measurement position in the potato models. **Figure 8** depicts the variations in impedance among different potato models. Notably, we conducted the impedance detection at a frequency of 400 Hz as the repetition frequency of the output pulse was 400 Hz. Therefore, the output energy was primarily

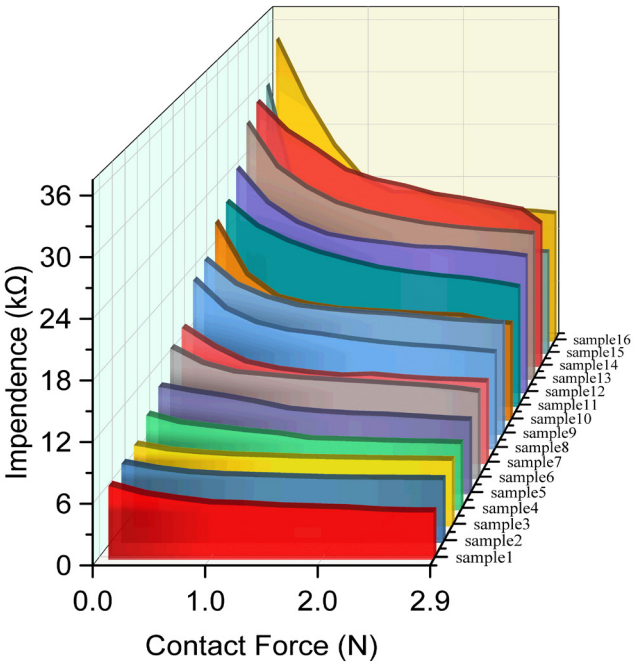

Figure 8. Contact impedance of different potato models under different contact forces.

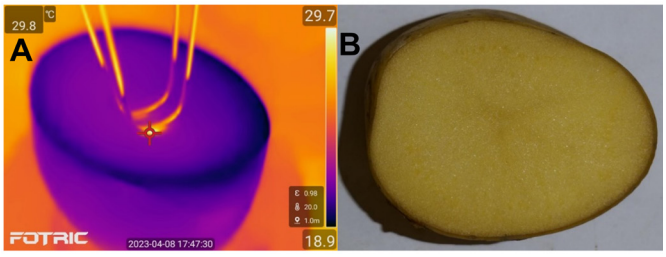

Figure 9. Thermal image and image of the control group. (A) Thermal image recorded during the experiment; (B) Control group with no pulse.

focused on the 400 Hz frequency in the spectrum.

In recent years, the IRE ablation technique has undergone rapid development in both clinical and basic research. The output pulse sequence in IRE has evolved from a monophasic pulse sequence to a biphasic pulse sequence. In current practice, monophasic and biphasic pulse sequences have become the most frequently used types of ablation pulse sequences [31-34]. Our study provides clear evidence that the efficacy of IRE is positively correlated with the CF between the electrode and potato tissue under both biphasic and monophasic output modes. Interestingly, while our results show no significant differences in the correlation for both monophasic and biphasic output modes, **Figure 6A** illustrates that the ablation area under monophasic output mode is greater than that under biphasic output mode at the same CF. The diminished efficacy of IRE ablation under the biphasic output mode could be attributed to the cancellation effect [35]. However, our potato model experiment conducted under current parameters did not reveal a significant difference in the efficacy of IRE ablation at CFs of 0.98 N and 0.49 N. This suggests that the present output electrical parameters may have saturated the IRE effect on the potato model. To mitigate the potential influence of the saturation trend in future experiments, we plan to reduce the pulses to 800 and use the biphasic output mode.

The output pulse amplitude is a critical electrical parameter for IRE, as it determines whether IRE can occur. Research has demonstrated that the electric field threshold for IRE in a potato model is approximately 475 V/cm, using a monophasic pulse sequence [36]. Literature suggests that reducing pulse width or using biphasic pulses results in an increased electric field threshold needed for tissue ablation, compared to monophasic or millisecond pulse width methods [30]. Therefore, in our experiment, we employed three voltage configurations: 350 V, 500 V, and 800 V, corresponding to electric field thresholds of 500 V/cm, 715 V/cm, and 1142 V/cm, respectively.

These voltage configurations are representative of three treatment scenarios in clinical and experimental settings: slightly above the IRE threshold, above the IRE threshold, and above twice the IRE threshold. Our study revealed that, in a fixed output mode (biphasic), the trend of increasing treatment efficacy along with increasing CF remains unchanged when only the output voltage is changed. Notably, we found no significant differences in this correlation across changes in amplitude. This suggests that during treatment, manipulation of the output voltage does not modify the dependence of treatment efficacy on CF.

Changes in the electrode-tissue coupling factor have a significant impact on the contact impedance between the electrode and the tissue. For instance, in a potato model, a loaded contact site will cause elastic deformation of the potato tissue within a specific load range [37, 38]. However, if the load surpasses that range, the potato tissue will undergo plastic deformation [37, 38]. Given that the rigidity of the electrode is substantially higher than that of the potato

tissue, when the electrode firmly contacts the potato tissue, the contact area between them will increase due to the elastic deformation of the potato tissue at the point of contact. Consequently, the contact impedance will decrease as the contact area increases. This phenomenon reinforces the need for proper electrode-tissue coupling in electroporation procedures to achieve desired outcomes. As the load is further increased, the cells at the contact point of the potato tissue begin to rupture, and the cellular fluid begins to seep out gradually, leading to a further increase in the contact area between the electrode and the tissue, as well as a subsequent decrease in contact impedance. The direct impact of the decrease in contact impedance is an increase in the output current. As a result, the increase in current leads to an increase in the oxidation area on the surface of the potato model, and results in a positive response of the potato surface oxidation area to the CF.

Overall, in the commonly used output configurations of IRE ablation pulses, there is a positive response of the treatment efficacy to the electrode-potato model CF in IRE.

Limitations

It is important to recognize the limitations of this study, which include the following:

1. The experiment was conducted only on a potato model, which may not accurately reflect the properties of human tissues.

2. The image processing was performed using an algorithm which selects pixels based on the difference between the RGB values of the reference and target regions. Therefore, noise generated during recording the potato oxidation areas may result in missed or erroneous detections. However, all potato models were photographed under the same light source, so this error is considered a systematic error and does not affect the trend analysis of the final data.

3. During the experiment, only the effects of biphasic and monophasic output modes at different output voltages were considered, while other potential factors that might affect the results were ignored, such as interphase interval, pulse frequency, and pulse width. However, although these potential factors can affect the IRE effect, their influence is limited due to the ensured consistency of the parameters across all experiments.

4. The experiment was conducted only on biphasic electrode configurations, so our results only apply to these configurations.

Conclusion

IRE ablation is a promising technology for treating AF because it offers several advantages over traditional catheter surgeries, including reduced thermal damage and reduced nerve damage caused by off-target treatment. Despite these advantages, the widespread clinical adoption of IRE for AF ablation is still hindered by several challenges, such as complex anesthesia protocols and ambiguous treatment outcomes that are influenced by multiple factors. These challenges must be addressed to ensure the efficacy and safety of IRE as a viable alternative to traditional catheter surgeries for AF ablation. The findings of this study indicate that the efficacy of IRE ablation in a potato model is positively correlated with the CF, regardless of whether the output pulse is biphasic or monophasic. Furthermore, our results demonstrate a positive correlation between CF and treatment efficacy under different output voltage amplitudes of a fixed biphasic mode. These observations highlight the importance of optimizing electrode-tissue coupling to achieve optimal outcomes in IRE ablation procedures. Our experimental findings have confirmed the importance of optimizing electrode-tissue coupling and highlight the need to consider the issue of electrode-tissue contact in the design of electrodes for IRE ablation. Poor electrode-tissue contact could lead to insufficient ablation, resulting in postoperative AF, underscoring the significance of improving electrode-tissue coupling for successful IRE ablation procedures. In addition, our experiment highlights the importance of considering the impact of coupling factors when conducting verification experiments on plant models. To further investigate the relationship between CF and treatment efficacy in IRE ablation, our future research will focus on animal models. These studies will provide more insights into the design of advanced IRE ablation protocols and facilitate the clinical promotion and translation of this technology for effective AF treatment.

References

[1] Zoni-Berisso M, Lercari F, Carazza T, et al. Epidemiology of atrial fibrillation: European perspective. Clin Epidemiol 2014;213-220.

[2] Rohrer U, Manninger M, Zirlik A, et al. Impact of Catheter Ablation for Atrial Fibrillation on Quality of Life. J Clin Med 2022;11:4541.

[3] Krijthe BP, Kunst A, Benjamin EJ, et al. Projections on the number of individuals with

atrial fibrillation in the European Union, from 2000 to 2060. Eur Heart J 2013;34:2746-2751.
[4] Andrade J, Khairy P, Dobrev D, et al. The clinical profile and pathophysiology of atrial fibrillation: relationships among clinical features, epidemiology, and mechanisms. Circ Res 2014;114:1453-1468.
[5] Rottner L, Bellmann B, Lin T, et al. Catheter ablation of atrial fibrillation: state of the art and future perspectives. Cardiol Ther 2020;9:45-58.
[6] Mulder BA, Rienstra M, Van Gelder IC, et al. Update on management of atrial fibrillation in heart failure: a focus on ablation. Heart 2022;108:422-428.
[7] Sanchis-Gomar F, Perez-Quilis C, Lippi G, et al. Atrial fibrillation in highly trained endurance athletes—description of a syndrome. Int J Cardiol 2017;226:11-20.
[8] Cappato R, Calkins H, Chen SA, et al. Updated worldwide survey on the methods, efficacy, and safety of catheter ablation for human atrial fibrillation. Circ Arrhythm Electrophysiol 2010;3:32-38.
[9] Pappone C, Oral H, Santinelli V, et al. Atrio-esophageal fistula as a complication of percutaneous transcatheter ablation of atrial fibrillation. Circulation 2004;109:2724-2726.
[10] Sacher F, Monahan KH, Thomas SP, et al. Phrenic nerve injury after atrial fibrillation catheter ablation: characterization and outcome in a multicenter study. J Am Coll Cardiol 2006;47:2498-2503.
[11] Wu TF, Tseng SY, Hung JCJItops. Generation of pulsed electric fields for processing microbes. IEEE Trans Plasma Sci 2004;32:1551-1562.
[12] Martens SL, Klein S, Barnes RA, et al. 600-ns pulsed electric fields affect inactivation and antibiotic susceptibilities of Escherichia coli and Lactobacillus acidophilus. AMB Express 2020;10:1-11.
[13] Wan J, Coventry J, Swiergon P, et al. Advances in innovative processing technologies for microbial inactivation and enhancement of food safety–pulsed electric field and low-temperature plasma. Trends Food Sci. Technol 2009;20:414-424.
[14] Guenther E, Klein N, Zapf S, et al. Prostate cancer treatment with Irreversible Electroporation (IRE): Safety, efficacy and clinical experience in 471 treatments. PLoS One 2019;14:e0215093.
[15] Reddy VY, Koruth J, Jais P, et al. Ablation of atrial fibrillation with pulsed electric fields: an ultra-rapid, tissue-selective modality for cardiac ablation. JACC Clin Electrophysiol 2018;4:987-995.
[16] Varghese F, Philpott JM, Neuber JU, et al. Surgical Ablation of Cardiac Tissue with Nanosecond Pulsed Electric Fields in Swine. Cardiovasc Eng Technol 2023;14:52-59.
[17] Loh P, van Es R, Groen MH, et al. Pulmonary vein isolation with single pulse irreversible electroporation: a first in human study in 10 patients with atrial fibrillation. Circ Arrhythm Electrophysiol 2020;13:e008192.
[18] Sugrue A, Vaidya VR, Livia C, et al. Feasibility of selective cardiac ventricular electroporation. PLoS One 2020;15:e0229214.
[19] Masnok K, Watanabe NJCE, Technology. Relationship of catheter contact angle and contact force with contact area on the surface of heart muscle tissue in cardiac catheter ablation. Cardiovasc Eng Technol 2021;12:407-417.
[20] Han M, Chen L, Aras K, et al. Catheter-integrated soft multilayer electronic arrays for multiplexed sensing and actuation during cardiac surgery. Nat Biomed Eng 2020;4:997-1009.
[21] Howard B, Verma A, Tzou WS, et al. Effects of Electrode-Tissue Proximity on Cardiac Lesion Formation Using Pulsed Field Ablation. Circ Arrhythm Electrophysiol 2022;15:e011110.
[22] Nakagawa H, Castellvi Q, Neal R, et al. B-PO03-131 effects of contact force on lesion size during pulsed field ablation. Heart Rhythm 2021;18:S242-S243.
[23] Soltani Sharif Abadi A, Alinaghi Hosseinabadi P, Hameed A, et al. Fixed-time observer-based controller for the human–robot collaboration with interaction force estimation. Int J Robust Nonlinear Control 2023.
[24] Shimachi S, Hirunyanitiwatna S, Fujiwara Y, et al. Adapter for contact force sensing of the da Vinci® robot. Int J Med Robot 2008;4:121-130.
[25] Abadi ASS, Ordys A, Pierscionek B. Controlling a Teleoperated Robotic Eye Surgical System Under a Communication Channel's Unknown Time Delay. 2023 27th International Conference on Methods and Models in Automation and Robotics (MMAR) 2023;211-215.
[26] Jeong S, Kim H, Park J, et al. Evaluation of electroporated area using 2, 3, 5-triphenyltetrazolium chloride in a potato model. Sci Rep 2021;11:20431.
[27] Lindelauf KH, Thomas A, Baragona M, et al. Plant-based model for the visual evaluation of electroporated area after irreversible electroporation and its comparison to in-vivo animal data. Sci Prog 2023;106:00368504231156294.
[28] Lv Y, Yao C, Rubinsky BJAoBE. A conceivable mechanism responsible for the synergy of high and low voltage irreversible electroporation pulses. Ann Biomed Eng 2019;47:1552-1563.
[29] Suchanek M, Olejniczak Z. Low field MRI study

of the potato cell membrane electroporation by pulsed electric field. J Food Eng 2018;231:54-60.

[30] Aycock KN, Zhao Y, Lorenzo MF, et al. A theoretical argument for extended interpulse delays in therapeutic high-frequency irreversible electroporation treatments. IEEE Trans Biomed Eng 2021;68:1999-2010.

[31] Charpentier KP, Wolf F, Noble L, et al. Irreversible electroporation of the liver and liver hilum in swine. HPB (Oxford) 2011;13:168-173.

[32] Yao C, Dong S, Zhao Y, et al. Bipolar microsecond pulses and insulated needle electrodes for reducing muscle contractions during irreversible electroporation. IEEE Trans Biomed Eng 2017;64:2924-2937.

[33] Sano MB, Arena CB, DeWitt MR, et al. In-vitro bipolar nano-and microsecond electropulse bursts for irreversible electroporation therapies. Bioelectrochemistry 2014;100:69-79.

[34] Wandel A, Ben-David E, Ulusoy BS, et al. Optimizing irreversible electroporation ablation with a bipolar electrode. J Vasc Interv Radiol 2016;27:1441-1450. e1442.

[35] Polajžer T, Dermol–Černe J, Reberšek M, et al. Cancellation effect is present in high-frequency reversible and irreversible electroporation. Bioelectrochemistry 2020;132:107442.

[36] Menegazzo I, Mammi S, Sgarbossa P, et al. Time Domain Nuclear Magnetic Resonance (TD-NMR) to evaluate the effect of potato cell membrane electroporation. Innovative Food Sci Emerging Technol 2020;65:102456.

[37] Sun W, Wu JM, Shi LR, et al. Simulation and Experiment of Mechanical Properties of Potato Compression. Adv Mater Res 2013;850–851:1303–1306.

[38] Konstankiewicz K, Zdunek AJIa. Influence of turgor and cell size on the cracking of potato tissue. Int Agrophys 2001;15.